Stochastic modeling of slip spatial complexities for the 1979 Imperial Valley, California, earthquake

Daniel Lavallée and Ralph J. Archuleta[1]

Institute for Crustal Studies, University of California, Santa Barbara, California, USA

Received 8 July 2002; revised 24 January 2003; accepted 6 February 2003; published 13 March 2003.

[1] Finite-fault source inversions reveal the spatial complexity of earthquake slip or prestress distribution over the fault surface. In this paper we discuss a stochastic model that reproduces the spatial variability and the long-range spatial correlation of the slip distribution of the 1979 Imperial Valley earthquake. We have found that stochastic models based on non-Gaussian distributions are better suited to describe the spatial variability of the slip amplitude over the fault. We also show that a stochastic modeling of the slip amplitude based on a Gaussian distribution fails to reproduce the spatial variability observed in the original slip distribution. The stochastic models can be used to deduce ground motion from other earthquakes statistically similar to Imperial Valley. *INDEX TERMS:* 3210 Mathematical Geophysics: Modeling; 7209 Seismology: Earthquake dynamics and mechanics; 7260 Seismology: Theory and modeling; 3250 Mathematical Geophysics: Fractals and multifractals. **Citation:** Lavallée, D., and R. J. Archuleta, Stochastic modeling of slip spatial complexities for the 1979 Imperial Valley, California, earthquake, *Geophys. Res. Lett.*, *30*(5), 1245, doi:10.1029/2002GL015839, 2003.

1. Introduction

[2] Earthquakes are complex phenomena [e.g., *Boatwright*, 1984]. An origin of complexity in earthquakes has been attributed to nonlinear effects in the friction law on the fault [*Carlson and Langer*, 1989]. On the other hand, *Rice* [1993] suggests geometric disorder of fault zones and fractal-like surface roughness of faults as the causal candidates responsible for seismic complexity. Even relatively simple models of faulting predict high spatial variability in stress drop over the fault [*Madariaga and Cochard*, 1994]. Although the origin of complexities in earthquake is still the object of debate, finite-fault source inversion of well recorded earthquakes reveal the complexity of both the slip and prestress spatial distribution over the fault surface. Evidence of the complex behavior was presented in papers by *Das and Aki* [1977], *Aki* [1979], *Day* [1982], and *Boatwright* [1984]. *Hartzell and Heaton* [1986] and *Beroza and Spudich* [1988] computed the rupture history of the Morgan Hill earthquake of 1984 and showed that the spatial distribution of slip over the fault surface was very heterogeneous. Regions of high slip alternate with regions where little slip occurred. Using near-source strong motion data to compile the prestress generated during a fault rupture for several recent earthquakes *Bouchon* [1997] concludes that a "consistent feature of the four earthquakes studied is the strong heterogeneity of the stress drop distribution over the fault." These studies also suggest that the spatial heterogeneity of the prestress is scale invariant (or self-similar). By scale invariant we mean that the spatial heterogeneity is statistically invariant under a change of scale length. These results are in good agreement with the observation that fault surface is also scale invariant and have asperities over a continuum of scale lengths [*Power and Tullis*, 1991].

2. Formulation of the Stochastic Model

[3] There are two basic hypotheses that underlie our study. First, a stochastic model can capture some of the main features of the heterogeneous spatial distribution of slip or prestress along the fault surface. Second, that the parameters of the stochastic model can be inferred, although indirectly and approximately, from a study of the statistical properties of the slip or prestress spatial distribution. The simple model proposed here consists of a convolution in the Fourier space between random variables (white noise) X and some function with power law dependence $k^{-\nu/2}$. The scaling exponent measures the departure from the non-correlated random variable (white noise); $k \equiv |\mathbf{k}|$ is the wave number magnitude. Such a stochastic model can be understood as a fractional Brownian motion that reduces to a random walk in its simplest manifestation—with $\nu = 2$ [see *Peitgen and Saupe*, 1988; *Falconer*, 1990]. Mathematically the stochastic model Y_x is given by the following relationship:

$$Y_x \propto \sum_{s=1}^{N} k^{-\nu/2} F_k[X] \exp[2\pi i(x-1)(s-1)/N] \qquad (1)$$

for a set of random variables X distributed over a one-dimensional lattice of length N. The sum in equation (1) goes from 1 to N; s is related to k by $k = 2\pi s$; $F_k[X]$ is the discrete Fourier transform of the random variables X, and x is the discrete position on the one-dimensional lattice. According to this, the power spectrum $P(k)$ associated to Y_x will be given by the following relation:

$$P(k) = |F_k[Y_x]|^2 \propto k^{-\nu} \qquad (2)$$

[4] In his seminal work on stochastic modeling of prestress spatial distribution, *Andrews* [1980] discussed a stochastic model based on the same formulation. In his model, there are two characteristic length scales, the depth of the brittle seismogenic region ($\sim 10^4$ m) and the grain

[1] Also at Department of Geological Sciences, University of California, Santa Barbara, California, USA.

0094-8276/03/2002GL015839$05.00

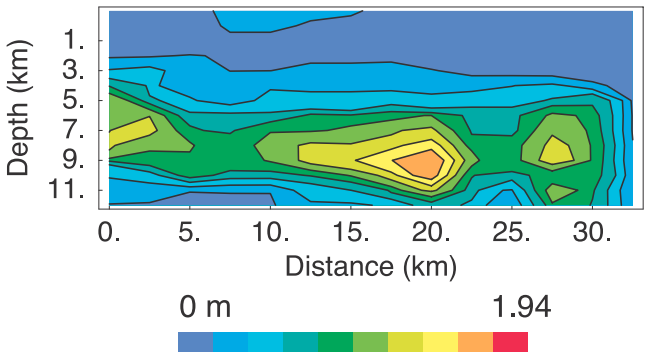

Figure 1. The spatial distribution of the slip parallel to strike for 1979 Imperial Valley earthquake is mapped onto the fault [*Archuleta*, 1984]. Contours of the slip illustrate the spatial heterogeneity.

size of the material ($\sim 10^{-2}$ m), bounding a continuum of length scales with no other characteristic length scale. Accordingly, a single model with the appropriate scaling property will reproduce the spatial complexities at every relevant length scale between these two characteristic length scales. A consequence of this formulation is that the slip and prestress spectral amplitudes have a functional behavior similar to the one given in equation (2). In Andrew's model, the white noise was generated with Gaussian random variables (J. Andrews, personal communication, 2001). *Von Seggen* [1981] and *Herrero and Bernard* [1994] adopted a similar view.

3. Stochastic Model for the 1979 Imperial Valley Earthquake Slip Spatial Distribution

[5] A faulting model of the 1979 Imperial Valley earthquake was determined by comparing synthetic particle velocity with near-source strong ground motion [*Archuleta*, 1984]. The spatial distribution of the slip was calculated at every 1.0 km along the downdip direction of the fault surface that extends from the surface to 13 km and at every 2.5 km along the strike that extends over 35 km (see Figure 1).

[6] The downdip resolution of the slip distribution is different from the horizontal resolution. For this reason we restrict the study of the spectral properties to the one-dimensional horizontal layers. This is the best way to study the spectral properties of the field using the information available without relying on interpolation techniques that can introduce some bias (see the discussion below). Each layer has 14 values. (We ignore the values at the ends; these values are all very small and close to zero.) The power spectrum $P(k)$ is computed for each of the 14 horizontal layers; from these the mean power spectrum of the 14 layers was estimated (Figure 2). The mean power spectrum follows a power law behavior with a scaling exponent close to minus one. This implies a power law behavior for long-range spatial correlation of the slip on the fault. The scaling properties and fractal dimensions of the slip distribution of several faults, including Imperial Valley, have also been examined by *Mai and Beroza* [2002]. However there are two important differences between their approach and ours in the procedure used to compute the power spectrum. First, they estimated the power spectrum a of 2D square lattice; second, they interpolated the slip distribution (see also Figure 2).

[7] Assuming that the slip spatial distribution S_x is equivalent to (or generated through) a stochastic model given by equation (1), we proceed to estimate the random variables X (white noise). The Fourier transform of the slip $F_k[S_x]$ is estimated for the fourteen horizontal layers that constitute the slip distribution illustrated in Figure 1. The random variables are given by:

$$X_x \propto F_x^{-1}\left[F_k[S_x] \times k^{\zeta}\right] \tag{3}$$

where F_x^{-1} is the Fourier inverse, S_x and x represent respectively the slip amplitude and the position along strike. The exponent ζ is chosen in such way that the mean power spectrum of X will have a scaling exponent close to zero. The mean is estimated over the 14 layers. The probability density function (PDF) associated with X is thus estimated.

[8] We then proceed to determine what theoretical model will provide a best fit to the PDF of X. Three candidates are considered: the Gauss distribution, the Cauchy distribution and the more general symmetric Lévy distribution [*Uchai-*

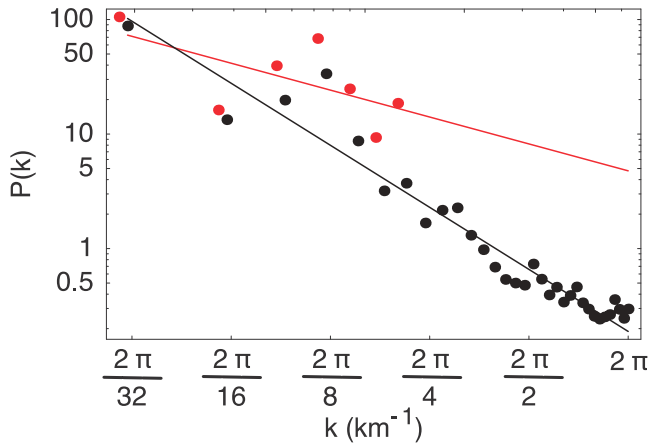

Figure 2. The mean power spectrum of slip for the fourteen horizontal layers is illustrated (red dots). The empirical trend of the power spectrum curve follows a power law behavior with a scaling exponent equal to −0.78. The power law is computed for scale lengths ranging from 5 km to 32.5 km. Fluctuations around the power law behavior can be attributed to a slow convergence to the theoretical curve—a behavior observed for stochastic models described in section 2. However, other mechanisms such as noise as well as uncertainties in computing the slip can also be responsible for the deviations. For comparison we also plot the curve of the mean power spectrum of the horizontal layers of the interpolated slip distribution (black dots). The best straight line (black) that fits the log-log curve of the power spectrum of the interpolated slip is −1.8. The slip spatial distribution was bilinearly interpolated to a 0.5 × 0.5 km grid. Note how the curve of the interpolated slip distribution separates from the curve of the original slip. In the physical space (slip on the fault), this difference implies that long-range spatial correlation is not handled properly. The small shift in the wave number observed between the two curves is due to the "discretization" in the Fourier space.

kin and Zolotarev, 1999]. The Lévy distribution is characterized by four parameters α, β, γ and μ. The parameter α, with $0 < \alpha \leq 2$, controls the rate of falloff of the tails of the PDF. The larger the value of α, the less likely it is to find a random variable far away from the central location. The case $\alpha = 2$ corresponds to the Gaussian law while $\alpha = 1$ (with $\beta = 0$) corresponds to the Cauchy law. The parameter β, with $-1 \leq \beta \leq 1$, controls the departure from symmetry of the PDF curve. When $\beta = 0$, the PDF is symmetric and centered about μ. The parameter γ, $\gamma > 0$, is mainly responsible for the PDF width whereas μ is the location or shift parameter of the PDF.

[9] For the three candidates, we have computed the model parameters that minimize the expression for the sum of the squared errors. The PDF of X and the best-fitting Gaussian, Cauchy and the symmetric Lévy PDF are illustrated in Figure 3. The best fit was obtained for the symmetric Lévy distribution: $\alpha = 0.92$, $\beta = 0$ (by default) $\gamma = 2.75$, and $\mu = -0.42$. However as shown in Figure 3 the Cauchy distribution (with $\alpha = 1$ by default) also provides a very good fit with $\gamma = 3.0$, and $\mu = -0.45$. Finally Figure 3 shows that the best fitting Gaussian distribution with standard deviation $\sigma = 4.48$, and $\mu = -0.57$ is a poor surrogate to the PDF of X.

[10] The difference between a Gaussian and non-Gaussian PDF has severe implications in the study and modeling of the slip distribution. The difference is illustrated by running the following numerical simulations. For the sake of simplicity, we assume here that the scaling properties of the slip are isotropic and used a formulation of the stochastic model similar to equation (1) but generalized over a two-dimensional lattice -see for instance *Peitgen and Saupe* [1988]. Using the estimated parameters of the Cauchy distribution given above, a 2D lattice of random variables is generated. (To be accurate, we must add that we used "truncated" Cauchy random variables, that is random variables with a spectrum of values bounded by the estimated minimum and maximum of X reported in Figure 3.) This set of variables is filtered in the Fourier space to produce a synthetic slip distribution (Figure 4) with the power spectrum corresponding to the original data. The same procedure is repeated but for a 2D lattice of Gaussian random variables generated with the parameters of the Gaussian curve presented in Figure 3. The synthetic slip based on a Gaussian distribution is illustrated in Figure 4. The two figures should be compared to the original slip distribution presented in Figure 1. In particular, note that the range of slip in Figure 4 (bottom graphic) is narrower than the range of values displayed in Figures 1 and 4 (top graphic). A stochastic model based on a Gaussian distribution that fits the PDF given in Figure 3 cannot generate the "extreme" slip events observed in the original slip distribution with amplitude close to 2 m, as observed in the original slip distribution. Asperities are usually defined as regions with large slip values on the fault, and the area occupied by asperities is related to the seismic moment through a power law [see *Somerville et al.*, 1999]. *Madariaga* [1979] derived a relationship between the seismic moment and a general heterogeneous stress drop distribution and the geometry of the fault. The numerical simulations indicate that a proper quantification of the slip underlying random variables is fundamental for a better understanding and description of the statistical properties

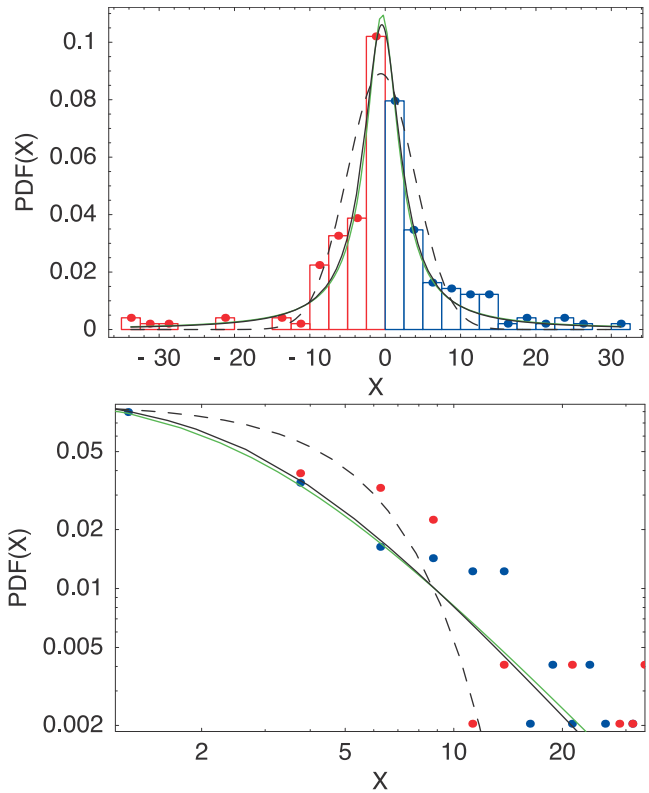

Figure 3. In the top graphic, the computed PDF of X (red and blue dots and bars) is compared to the Lévy PDF, (green curve), the Cauchy PDF (black curve) and the Gaussian PDF (dashed curve) that best fit the PDF of X—the slip amplitude. The left tail is red while the right tail is in blue with X corresponding to the magnitude of the random variables. The increment ΔX used to compute the PDF—and corresponding to the width of the bar—is set to 2.5. The bottom graphic provides the same information but on a log-log plot. The Lévy and Cauchy probability density functions are characterized by a tail that drops according to a power law that is best illustrated on a log-log plot. The Gaussian PDF fails to reproduce the functional behavior of the computed PDF. According to the Gaussian PDF, the large slip events have almost a zero probability of being observed. The consequences and predictions associated with the asymptotic behavior of Gaussian and non-Gaussian distributions are discussed in the text and illustrated in Figure 4. The results presented in these graphics are not significantly modified when the PDF is computed with the increment $\Delta X = 1.25$.

and long-range spatial correlation of asperities as well as the evaluation of the seismic moment based on the asperity or prestress spatial distribution.

[11] Although still an oddity in seismology, observations of a non-Gaussian distribution have been reported in the literature. For instance, the analysis of the statistical properties of strong ground motion recorded in the epicentral areas of large earthquake have shown that the peak acceleration distribution is non-Gaussian [*Gusev*, 1996], characterized by "heavy tailed" distribution (a typical signature of Lévy distribution as illustrated in Figure 3) and are better approximated by Cauchy distribution (with $\alpha = 1$) [*Tumar-*

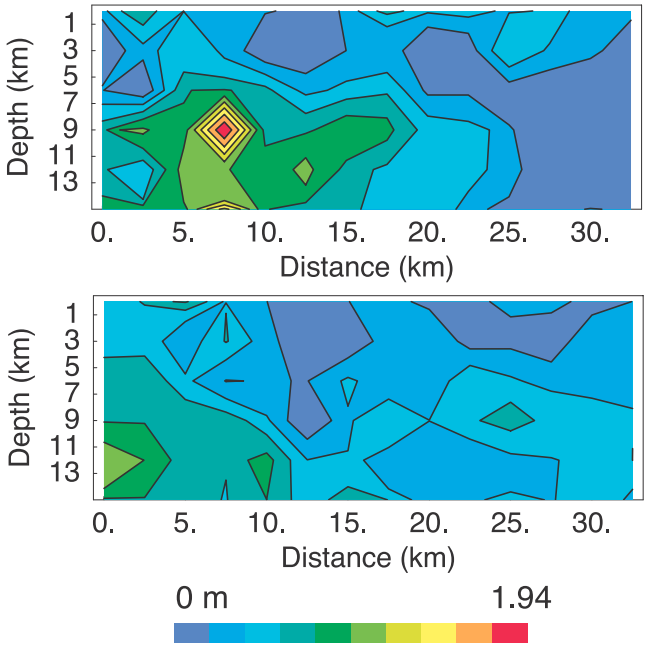

Figure 4. In the top graphic, the synthetic slip is generated using the two-dimensional fields of filtered Cauchy random variables. In term of spatial variability, the synthetic field compares well with the original data illustrated in Figure 1 except for regions close to the surface. In the bottom graphic, the synthetic slip is generated using the two-dimensional fields of filtered Gaussian random variables. Note that the inter-variability of the synthetic slip based on a Gaussian description fails to reproduce the variability observed in the original data (Figure 1). It should be noted also that choosing a realization with a weak slip distribution near the top is just a convenient choice to enhance the similarity with Figure 1. The stochastic model doesn't differentiate between this realization and the same realization rotated by 180°.

kin and Archuleta, 1997]. This suggests that observation of non-Gaussian distribution in the strong ground motion records may have its origin in the spatial distribution of slip over the fault surface. Using a multiasperity fault model, *Gusev* [1989] has postulated that local stress drop values will be governed by Lévy distribution.

4. Conclusion

[12] In this paper, we investigated the spatial variability of the slip distribution of the 1979 Imperial Valley earthquake. We have shown that interpolation of the slip spatial distribution—a common procedure in numerical computation of rupture propagation—introduces spurious long-range spatial correlations. We also proposed a stochastic model—based on non-Gaussian distribution—that reproduces the main features of the slip spatial variability, including the presence of large values of slip. These results suggest that the heterogeneous spatial slip distribution of Imperial Valley is one realization of a stochastic model. This implies that by describing the statistical properties of earthquakes we can lay the foundation for equivalent scenario earthquakes. This will allow computation of ground motion for a range of earthquakes all of which will have the same inherent statistical properties.

[13] **Acknowledgments.** We acknowledge fruitful discussions with Y. Ben-Zion and S. M. Day for issues regarding interpolation of the data. We appreciate the thoughtful comments of the reviewers who have helped to clarify the contents of this paper. Computations were performed using *Mathematica* 4.1 (Wolfram Research, Inc., 1999). This research has been supported by SCEC grant No. 572726 as well as UCSB matching funds for SCEC and KECK grant No. 19990997. This is ICS contribution No. 0554.

References

Aki, K., Characterization of barriers of an earthquake fault, *J. Geophys. Res.*, *84*, 6140–6148, 1979.
Andrews, D. J., A stochastic fault model, 1, Static case, *J. Geophys. Res.*, *78*, 3867–3877, 1980.
Archuleta, R. J., A faulting model for the 1979 Imperial Valley earthquake, *J. Geophys. Res.*, *89*, 4559–4585, 1984.
Beroza, G. C., and P. Spudich, Linearized inversion for fault rupture behavior: Application to the 1984 Morgan Hill, California, earthquake, *J. Geophys. Res.*, *93*, 6275–6296, 1988.
Boatwright, J., The effect of rupture complexity on estimates of source size, *J. Geophys. Res.*, *89*, 1132–1146, 1984.
Bouchon, M., The state of stress on some faults of the San Andreas system as inferred from near-field strong motion data, *J. Geophys. Res.*, *102*, 11,731–11,744, 1997.
Carlson, J. M., and J. S. Langer, Mechanical model of an earthquake fault, *Phys. Rev. A*, *40*, 6470–6484, 1989.
Das, S., and K. Aki, A numerical study of two-dimensional spontaneous rupture propagation, *Geophys, J. R. Astron. Soc.*, *50*, 643–668, 1977.
Day, S. M., Three-dimensional simulation of spontaneous rupture: The effect of non-uniform prestress, *Bull. Seismol. Soc. Am.*, *72*, 1881–1902, 1982.
Falconer, K., *Fractal Geometry*, 288 pp., John Wiley, New York, 1990.
Gusev, A., On relations between earthquake population and asperity population on a fault, *Tectonophysics*, *211*, 85–98, 1989.
Gusev, A., Peak factors of Mexican accelerograms: Evidence of a non-Gaussian amplitude distribution, *J. Geophys. Res.*, *101*, 20,083–20,090, 1996.
Hartzell, S. H., and T. H. Heaton, Rupture history of the 1984 Morgan Hill, California, earthquake from the inversions of strong ground motion records, *Bull. Seismol. Soc. Am.*, *76*, 649–674, 1986.
Herrero, A., and P. Bernard, A kinematic self-similar rupture process for earthquake, *Bull. Seismol. Soc. Am.*, *84*, 1216–1228, 1994.
Madariaga, R., On the relation between seismic moment and stress drop in the presence of stress and strength heterogeneity, *J. Geophys. Res.*, *84*, 2243–2250, 1979.
Madariaga, R., and A. Cochard, Seismic source dynamics, heterogeneity and friction, *Ann. Geofis.*, *37*, 1349–1375, 1994.
Mai, P. M., and G. C. Beroza, A spatial random-field model to characterize complexity in earthquake slip, *J. Geophys. Res.*, *107*(B11), 2308, doi:10.1029/2001JB000588, 2002.
Peitgen, H.-O., and D. Saupe, *The Science of Fractal Images*, 312 pp., Springer-Verlag, New York, 1988.
Power, W. L., and T. E. Tullis, Euclidean and fractal models for the detection of rock surface roughness, *J. Geophys. Res.*, *93*, 415–424, 1991.
Rice, J. R., Spatio-temporal complexity of slip on a fault, *J. Geophys. Res.*, *98*, 9885–9907, 1993.
Somerville, P., K. Irikura, R. Graves, S. Sawata, D. Wald, N. Abrahamson, Y. Iwasaki, T. Kagawa, N. Smith, and A. Kowada, Characterizing crustal earthquake slip model for the prediction of strong ground motion, *Seismol. Res. Lett.*, *70*, 59–80, 1999.
Tumarkin, A. G., and R. J. Archuleta, Stochastic ground motion modeling revisited, *Seismol. Res. Lett.*, *68*, 312, 1997.
Uchaikin, V. V., and V. M. Zolotarev, *Chance and Stability*, 570 pp., VSP, Utrecht, Netherlands, 1999.
Von Seggen, D., A random stress model for seismicity statistics and earthquake prediction, *Geophys. Res. Lett.*, *7*, 637–640, 1981.

D. Lavallée and R. J. Archuleta, Institute for Crustal Studies, University of California, Santa Barbara, CA 93106, USA. (daniel@crustal.ucsb.edu; ralph@crustal.ucsb.edu)